

ON THE ORDER OF ACCURACY FOR FINITE DIFFERENCE APPROXIMATIONS OF PARTIAL DIFFERENTIAL EQUATIONS USING STENCIL COMPOSITION

ABHISHEK MISHRA, DAVID SALAC AND MATTHEW G. KNEPLEY

Institute for Computational and Data Sciences, University at Buffalo

ABSTRACT. Stencil composition uses the idea of function composition, wherein two stencils with arbitrary orders of derivative are composed to obtain a stencil with a derivative order equal to sum of the orders of the composing stencils. In this paper, we show how stencil composition can be applied to form finite difference stencils in order to numerically solve partial differential equations (PDEs). We present various properties of stencil composition and investigate the relationship between the order of accuracy of the composed stencil and that of the composing stencils. We also present numerical experiments wherein we verify the order of accuracy by convergence tests. To demonstrate an application to PDEs, a boundary value problem involving the two-dimensional biharmonic equation is numerically solved using stencil composition and the order of accuracy is verified by performing a convergence test.

KEYWORDS. stencil, finite-difference, order-of-accuracy, composition, weights, biharmonic

1. INTRODUCTION

Partial differential equations (PDEs) have a wide variety of applications, ranging from engineering [19] to biology [16], as well as in machine learning applications such as image processing [21]. The first step in numerically solving any such PDE requires a discretization technique which replaces the continuous equation by a discrete algebraic equation [2]. The discretization technique involves approximating the derivative terms in the PDE by a numerical method such as the finite difference [1, 7, 22], finite element [3, 11, 12], or finite volume method [5, 10, 20], calculated at discrete points, or in other words, the grid points.

In this work we focus on the finite difference method, where a linear PDE is discretized at a central point via a linear combination of neighboring points. This combination of neighboring points and their associated weights is called a *stencil*. For PDEs, stencils at points are coupled to the stencils at neighboring points, which leads to a coupled set of linear equations if the function is unknown. In particular, we are interested in situations where the PDE itself is written as a repeated series of derivatives, such as the biharmonic equation which can be stated as two applications of the Laplace operator, $\Delta\Delta u$, or where the method chosen to solve a PDE results from the multiple applications of operators. An example of the latter is the Closest Point Method (CPM), which is a technique to solve surface differential equations on embedded surfaces whereby interpolation and derivative stencils are combined [15, 4]. The CPM uses the fact that if the solution on an embedded surface, such as those described by the level-set method [14, 8], is extended into the embedding space such that it is constant in the direction normal to the surface, then standard Cartesian derivatives will correspond to surface derivatives when interpolated back down to the surface. This allows for linear systems to be created that allows for the solution of differential equations on arbitrary surfaces in a systematic manner.

In both cases (biharmonic or CPM) the end result can be written as a series of (typically) sparse matrix-matrix products. For many reasons (numerical stability, linear system solver speed, memory pre-allocation, etc) it is often advantageous to obtain a single matrix representing these types of systems. The naive method would be to use each individual stencil to create individual matrices in memory and perform many matrix-matrix products. For very large systems it is necessary to have some information on the sparsity pattern of the resulting matrix, which is difficult to obtain for arbitrary systems. It would be advantageous to have a stencil of the final system *before* the matrix is formed. This leads to the concept of *stencil composition*, whereby one stencil is *composed* with another stencil. Focusing on the composition of derivative stencils, this allows (for example) two stencils with arbitrary derivative orders of \bar{a} and \bar{b} to be composed to obtain a stencil with a derivative order of $\bar{a} + \bar{b}$. This composed stencil can then be used to create the matrix required for solution of the PDE. In this work we explore the use of stencil composition of lower-order derivative stencils to form a single higher-order derivative stencil. In addition to demonstrating that resultant stencil

does approximate the desired derivative, we will also demonstrate that if the order of accuracy of these two stencils are p and q then the order of accuracy for the resulting stencil will be $\min(p, q)$.

The remainder of this paper is organized as follows. In section 2.1, we formulate the shorthand notation for the finite difference stencil using the Taylor series, encapsulated as a vector. This notation is demonstrated by deriving the first-order and second-order derivative stencils using this vector. In section 2.2, the concept of stencil composition is introduced. The associativity of stencil composition is shown and the order of accuracy is investigated. Section 2.3 extends the concept of stencil composition and its order of accuracy to higher-dimensions. Sections 3.1 and 3.2 present numerical examples using some arbitrary functions in one and two dimensions respectively, along with convergence studies. Section 3.3 demonstrates the PDE application of stencil composition by numerically solving a biharmonic boundary value problem, and verifying the order of accuracy by performing a convergence test. Lastly, in section 4, we draw some conclusions and discuss possible usage and applications of stencil composition.

2. NUMERICAL DISCRETIZATION

2.1. Finite Difference Stencils. In this section the notation used in the remainder of this work is outlined. Let $f(\mathbf{x})$ be a function defined over a lattice in \mathbb{R}^d . We define the *target* point \mathbf{x}_0 as the location where we wish to evaluate the function f or some derivative of the function. In general the target point does not need to lie on the lattice, but generally will for derivative approximations, which is the assumption here. We define a *source* point $\mathbf{x}_i \neq \mathbf{x}_0$ and can estimate the value of the function at the source point via a Taylor series centered at the target point,

$$(1) \quad f(\mathbf{x}_i) = f(\mathbf{x}_0) + (\mathbf{x}_i - \mathbf{x}_0)^T \{Df(\mathbf{x}_0)\} + \frac{1}{2!} (\mathbf{x}_i - \mathbf{x}_0)^T \{D^2 f(\mathbf{x}_0)\} (\mathbf{x}_i - \mathbf{x}_0) + \dots$$

where $Df(\mathbf{x}_0)$ is the gradient of $f(x)$ and $D^2 f(\mathbf{x}_0)$ is the Hessian, both evaluated at \mathbf{x}_0 .

Assuming that both target and source points lie on a regular lattice with spacing h , we can represent the difference using the integer vector $\mathbf{u}_i \in \mathbb{Z}^d$, so that

$$(2) \quad \mathbf{x}_i - \mathbf{x}_0 = h\mathbf{u}_i.$$

We can then rewrite the series expansion (1) using multi-index notation,

$$(3) \quad f(\mathbf{x}_i) = \sum_{|\alpha| \geq 0} h^\alpha \frac{\mathbf{u}_i^\alpha}{\alpha!} f^{(\alpha)}(\mathbf{x}_0),$$

where \mathbf{u}_i^α refers to component-wise powers. Let us introduce an integer β , which represents the shift of derivatives in any given direction,

$$(4) \quad f^{(\beta)}(\mathbf{x}_i) = \sum_{|\alpha| \geq 0} h^\alpha \frac{\mathbf{u}_i^\alpha}{\alpha!} f^{(\alpha+\beta)}(\mathbf{x}_0).$$

Therefore, when $\beta = 0$ we get (3) and the Taylor series expansion (1). For $\beta > 0$ this results in a Taylor series of the β^{th} -derivative of $f(\mathbf{x}_i)$. We can now compactly write this infinite series using the following notation,

$$(5) \quad f^{(\beta)}(\mathbf{x}_i) \longrightarrow (\mathbf{S}_i, \beta),$$

where (\mathbf{S}_i, β) denotes the Taylor Series expansion of a single source point centered at the target point, and the infinite vector \mathbf{S}_i contains the coefficients associated with each $h^\alpha \mathbf{s}_{i,\alpha} f^{(\alpha+\beta)}$:

$$(6) \quad (\{1, 1, \frac{1}{2!}, \frac{1}{3!}, \dots\}, \beta = 0) = f(\mathbf{x}_0) + hf'(\mathbf{x}_0) + \frac{1}{2!} h^2 f''(\mathbf{x}_0) + \frac{1}{3!} h^3 f^{(3)}(\mathbf{x}_0) + \dots$$

while

$$(7) \quad (\{0, 1, 1, \frac{1}{2!}, \frac{1}{3!}, \dots\}, \beta = 0) = hf'(\mathbf{x}_0) + h^2 f''(\mathbf{x}_0) + \frac{1}{2!} h^3 f^{(3)}(\mathbf{x}_0) + \frac{1}{3!} h^4 f^{(4)}(\mathbf{x}_0) + \dots$$

for a one-dimensional system with $u = 1$. It must be noted that, if we divide \mathbf{S}_i by h^p , the coefficients in the infinite vector \mathbf{S}_i move p slots to the left, and the β increases by p . For instance, dividing (7) by h shifts the coefficients left one slot and increases β by one,

$$(8) \quad (\{1, 1, \frac{1}{2!}, \frac{1}{3!}, \dots\}, \beta = 1) = f'(\mathbf{x}_0) + hf''(\mathbf{x}_0) + \frac{1}{2!} h^2 f^{(3)}(\mathbf{x}_0) + \frac{1}{3!} h^3 f^{(4)}(\mathbf{x}_0) + \dots$$

The sequences centered at a given target point constitute a vector space, and thus it is possible to take linear combinations of n -different source points.

Definition 1. A finite difference stencil approximating the p^{th} -derivative of $f^{(\beta)}(\mathbf{x}_0)$ with associated scalar weights $a_i \propto h^{-p}$, can be expressed using the following notation

$$(9) \quad \begin{aligned} f^{(\beta+p)}(\mathbf{x}_0) &\approx \sum_i a_i f^{(\beta)}(\mathbf{x}_i) = \sum_i a_i \left(\sum_{|\alpha| \geq 0} h^\alpha \frac{\mathbf{u}_i^\alpha}{\alpha!} f^{(\alpha+\beta)}(\mathbf{x}_0) \right) \\ &\longrightarrow \sum_i a_i (\mathbf{S}_i, \beta) = (\mathbf{T}, \beta + p) = (\mathbf{T}, \bar{\beta}), \end{aligned}$$

where, $\bar{\beta}$ indicates the increase in β when weights are applied and the overall derivative order approximated.

This can be alternatively written as

$$(10) \quad t_\alpha = \sum_{|\alpha| \geq 0} \sum_i a_i \frac{\mathbf{u}_i^\alpha}{\alpha!} \text{ such that } \sum_{|\alpha| \geq 0} t_\alpha h^\alpha f^{(\alpha+\beta)}(\mathbf{x}_0) \longrightarrow (\mathbf{T}, \bar{\beta}),$$

where t_α denotes the coefficient associated with h^α . The remainder of this work assumes that whenever the notation \mathbf{T} is used, stencil weights have already been applied. The symbol $\bar{\beta}$ may thus be suppressed and stencil may be expressed using (\mathbf{T}, β) .

Definition 2. A finite difference stencil expressed using the notation $(\mathbf{T}, \beta + p)$ approximating a $(\beta + p)^{\text{th}}$ -order derivative with an order of accuracy q , must satisfy the following:

- all coefficients associated with derivatives of order less than $\beta + p$ in a weighted sum of the Taylor series must go to zero, and thus,
- the first element in \mathbf{T} must be equal to one, which represents the coefficient of the $(\beta + p)^{\text{th}}$ derivative. Therefore,
- the value of $\beta + p$ indicates what derivative order the stencil approximates. Moreover,
- all coefficients associated with derivatives of order greater than $\beta + p$ and less than $\beta + p + q$ must be equal to zero, and
- the coefficient associated with order of derivative $\beta + p + q$ must be non-zero.

It is important to note that the first non-zero value that follows the first element in \mathbf{T} provides the coefficient associated with the order of accuracy, q , as demonstrated below.

2.1.1. First Derivative Stencil. We will begin with an example in one dimension. The simplest approximation we can make is to use an evaluation to estimate the value of the target point, x_0 , itself,

$$(11) \quad f(x_0) \longrightarrow (\{1, 0, 0, \dots\}, \beta = 0) = (\mathbf{S}_0, \beta = 0).$$

Next, we could move our source evaluation point x forward one lattice spacing $x_1 = x_0 + h$,

$$(12) \quad f(x_1) \longrightarrow (\{1, 1, \frac{1}{2!}, \frac{1}{3!}, \dots\}, \beta = 0) = (\mathbf{S}_1, \beta = 0),$$

or one step backward $x_{-1} = x_0 - h$,

$$(13) \quad f(x_{-1}) \longrightarrow (\{1, -1, \frac{1}{2!}, \frac{-1}{3!}, \dots\}, \beta = 0) = (\mathbf{S}_{-1}, \beta = 0).$$

Each of these is an $\mathcal{O}(h)$ approximation to $f(x_0)$ as

$$(14) \quad f(x_0) - f(x_1) \longrightarrow (\{0, -1, \frac{-1}{2!}, \dots\}, \beta = 0),$$

$$(15) \quad f(x_0) - f(x_{-1}) \longrightarrow (\{0, 1, \frac{1}{2!}, \dots\}, \beta = 0),$$

and the first non-vanishing term is proportional to $hf'(x_0)$.

Applying first derivative weights $\mathbf{a} = \left(\frac{1}{2h}, \frac{-1}{2h}\right)$ to $\mathbf{S} = (\mathbf{S}_1, \mathbf{S}_{-1})$ from (12) and (13) we get

$$\begin{aligned}
 \sum_i a_i(\mathbf{S}_i, \beta) &= \frac{1}{2h}(\mathbf{S}_1, \beta = 0) - \frac{1}{2h}(\mathbf{S}_{-1}, \beta = 0) \\
 &= \frac{1}{2h}(\{1, 1, \frac{1}{2!}, \frac{1}{3!}, \dots\}, \beta = 0) - \frac{1}{2h}(\{1, -1, \frac{1}{2!}, \frac{-1}{3!}, \dots\}, \beta = 0) \\
 &= \frac{1}{2h}(\{0, 2, 0, \frac{2}{3!}, 0, \dots\}, \beta = 0) = (\{1, 0, \frac{1}{6}, 0, \dots\}, \beta = 1) \\
 &\rightarrow (\mathbf{T}, \beta = 1).
 \end{aligned}
 \tag{16}$$

Since the first element of \mathbf{T} is one, $\beta = 1$ therefore indicates that the stencil is an approximation of $f'(x_0)$. As the first non-zero value following the first element in \mathbf{T} in the vector is in the location corresponding to h^2 this approximation is of order $\mathcal{O}(h^2)$.

The numerical approximation can thus be written in the following manner,

$$f'(x_0) \rightarrow \frac{f(x_1) - f(x_{-1})}{2h} + \mathcal{O}(h^2). \tag{17}$$

2.1.2. Second Derivative Stencil. The second derivative can be approximated in a similar manner. In this case the stencil must zero out the coefficients associated with $f(x_0)$ and $f'(x_0)$, and result in a coefficient of one associated with $f''(x_0)$. Applying the weights $\mathbf{a} = \left(\frac{1}{h^2}, \frac{-2}{h^2}, \frac{1}{h^2}\right)$ to $\mathbf{S} = (\mathbf{S}_1, \mathbf{S}_0, \mathbf{S}_{-1})$ we obtain

$$\begin{aligned}
 \sum_i a_i(\mathbf{S}_i, \beta) &= \frac{1}{h^2}(\mathbf{S}_1, \beta = 0) - \frac{2}{h^2}(\mathbf{S}_0, \beta = 0) + \frac{1}{h^2}(\mathbf{S}_{-1}, \beta = 0) \\
 &= \frac{1}{h^2}(\{1, 1, \frac{1}{2!}, \frac{1}{3!}, \dots\}, \beta = 0) - \frac{2}{h^2}(\{1, 0, 0, 0, \dots\}, \beta = 0) \\
 &\quad + \frac{1}{h^2}(\{1, -1, \frac{1}{2!}, \frac{-1}{3!}, \dots\}, \beta = 0) \\
 &= \frac{1}{h^2}(\{0, 0, 1, 0, \frac{1}{12}, \dots\}, \beta = 0) = (\{1, 0, \frac{1}{12}, \dots\}, \beta = 2) \\
 &\rightarrow (\mathbf{T}, \beta = 2).
 \end{aligned}
 \tag{18}$$

Clearly this is now an $\mathcal{O}(h^2)$ approximation to $f''(x_0)$.

2.2. Stencil Composition. We now introduce the concept of stencil composition, which makes use of the idea of function compositions. Just like a function composition, stencil composition is an operation which takes two stencils A and B , with derivative orders of \bar{a} and \bar{b} respectively, and generates a stencil C such that $C = B(A)$ with a derivative order of $\bar{a} + \bar{b}$. In this operation, the outer stencil B is applied to the result obtained by applying the inner stencil A to any function f . To formally introduce this concept let the two stencils be given as

$$A = \sum_i a_i f^{(\beta)}(\mathbf{x}_i) = \sum_i a_i \left(\sum_{|\alpha| \geq 0} h^\alpha \frac{\mathbf{u}_i^\alpha}{\alpha!} f^{(\alpha+\beta)}(\mathbf{x}_0) \right) \tag{19}$$

and

$$B = \sum_j b_j g^{(\gamma)}(\mathbf{x}_j) = \sum_j b_j \left(\sum_{|\alpha| \geq 0} h^\alpha \frac{\mathbf{v}_j^\alpha}{\alpha!} g^{(\alpha+\gamma)}(\mathbf{x}_0) \right), \tag{20}$$

where the source points, $\mathbf{x} = \mathbf{x}_0 + h\mathbf{u}$ and $\mathbf{x} = \mathbf{x}_0 + h\mathbf{v}$, and the associated weights, $\mathbf{a} \propto h^{-\bar{a}}$ and $\mathbf{b} \propto h^{-\bar{b}}$, could differ between the two stencils. For composition, the outer stencil, B in this case, is written as working on function values, not derivatives, and therefore $\gamma = 0$. The composition can then be written as

$$\begin{aligned}
 C = B(A) &= \sum_j b_j \sum_i a_i f^{(\beta)}(\mathbf{x}_i + \mathbf{x}_j) = \sum_j \sum_i a_i b_j \left(\sum_{|\alpha| \geq 0} h^\alpha \frac{(\mathbf{u}_i + \mathbf{v}_j)^\alpha}{\alpha!} f^{(\alpha+\beta)}(\mathbf{x}_0) \right) \\
 &\rightarrow \sum_j \sum_i a_i b_j (\mathbf{S}_{i+j}, \beta) = (\mathbf{T}, \bar{\beta} = \beta + \bar{a} + \bar{b}).
 \end{aligned}
 \tag{21}$$

As an example, we will derive a second derivative stencil using the composition of two first derivative stencils. As a reminder, the first derivative stencil (17) looks like

$$f'(x_0) \longrightarrow \frac{f(x_1) - f(x_{-1})}{2h} + \mathcal{O}(h^2),$$

and therefore $\mathbf{u} = \{1, -1\} = \mathbf{v}$ is the associated integer vector and $\mathbf{a} = \{1/(2h), -1/(2h)\} = \mathbf{b}$ are the stencil weights. Note that as we will be composing a stencil with itself, the integer vectors/weights of both the inner and outer stencil will be the same and $\beta = 0$. The composition is then

$$\begin{aligned} B(A) &= \sum_j \sum_i a_i b_j \left(\sum_{|\alpha| \geq 0} h^\alpha \frac{(\mathbf{u}_i + \mathbf{v}_j)^\alpha}{\alpha!} f^{(\alpha)}(\mathbf{x}_0) \right) \\ &= \sum_j b_j \left[\frac{1}{2h} \left(\sum_{|\alpha| \geq 0} h^\alpha \frac{(1 + \mathbf{v}_j)^\alpha}{\alpha!} f^{(\alpha)}(\mathbf{x}_0) \right) \right. \\ &\quad \left. - \frac{1}{2h} \left(\sum_{|\alpha| \geq 0} h^\alpha \frac{(-1 + \mathbf{v}_j)^\alpha}{\alpha!} f^{(\alpha)}(\mathbf{x}_0) \right) \right] \\ &= \frac{1}{2h} \left[\frac{1}{2h} \left(\sum_{|\alpha| \geq 0} h^\alpha \frac{2^\alpha}{\alpha!} f^{(\alpha)}(\mathbf{x}_0) \right) - \frac{1}{2h} \left(\sum_{|\alpha| \geq 0} h^\alpha \frac{0^\alpha}{\alpha!} f^{(\alpha)}(\mathbf{x}_0) \right) \right] \\ &\quad - \frac{1}{2h} \left[\frac{1}{2h} \left(\sum_{|\alpha| \geq 0} h^\alpha \frac{0^\alpha}{\alpha!} f^{(\alpha)}(\mathbf{x}_0) \right) - \frac{1}{2h} \left(\sum_{|\alpha| \geq 0} h^\alpha \frac{(-2)^\alpha}{\alpha!} f^{(\alpha)}(\mathbf{x}_0) \right) \right] \\ &= \frac{1}{4h^2} \left[\sum_{|\alpha| \geq 0} \left(h^\alpha \frac{2^\alpha + (-2)^\alpha}{\alpha!} f^{(\alpha)}(\mathbf{x}_0) \right) - 2f(\mathbf{x}_0) \right] \\ (22) \quad &\longrightarrow \frac{1}{4h^2} (\{0, 0, 4, 0, \frac{4}{3}, \dots\}, \beta = 0) = (\{1, 0, \frac{1}{3}, \dots\}, \beta = 2) \end{aligned}$$

where $0^0 = 1$. From this it is clear that this is a $\mathcal{O}(h^2)$ approximation to $f''(x_0)$.

This can be verified by computing the stencil composition of coefficients given by (21). In this case we have

$$(23) \quad B(A) = \sum_j \sum_i a_i b_j f(\mathbf{x}_i + \mathbf{y}_j) = \frac{1}{4h^2} (f(x_{-2}) - 2f(x_0) + f(x_2))$$

where, $x_2 = x_0 + 2h$ and $x_{-2} = x_0 - 2h$. The expansion vectors of $f(x_2)$ and $f(x_{-2})$ can be written as

$$(24) \quad f(x_2) \longrightarrow (\{1, 2, 2, \frac{4}{3}, \frac{2}{3}, \dots\}, \beta = 0),$$

$$(25) \quad f(x_{-2}) \longrightarrow (\{1, -2, 2, \frac{-4}{3}, \frac{2}{3}, \dots\}, \beta = 0).$$

Inserting the stencil vectors into (23) results in

$$\begin{aligned} B(A) &= \frac{1}{4h^2} \left[(\{1, 2, 2, \frac{4}{3}, \frac{2}{3}, \dots\}, \beta = 0) + (\{1, -2, 2, \frac{-4}{3}, \frac{2}{3}, \dots\}, \beta = 0) \right. \\ &\quad \left. - 2(\{1, 0, 0, 0, \dots\}, \beta = 0) \right] \\ (26) \quad &= \frac{1}{4h^2} (\{0, 0, 4, 0, \frac{4}{3}, \dots\}, \beta = 0) = (\{1, 0, \frac{1}{3}, \dots\}, \beta = 2), \end{aligned}$$

which matches the previous result.

2.2.1. Associativity.

Lemma 1. *Stencil composition follows the rule of associativity, i.e., no matter how we compose the two stencils A and B , with order of derivatives \bar{a} and \bar{b} respectively, the composed stencil $C = A(B) = B(A)$ is equal with a derivative order of $\bar{a} + \bar{b}$.*

Proof. Using the stencils A and B previously defined in (19) and (20),

$$\begin{aligned} B(A) &= \sum_j b_j \sum_i a_i f^{(\beta)}(\mathbf{x}_i + \mathbf{x}_j) = \sum_j \sum_i a_i b_j f^{(\beta)}(\mathbf{x}_i + \mathbf{x}_j) = \sum_i \sum_j a_i b_j f^{(\beta)}(\mathbf{x}_i + \mathbf{x}_j) \\ (27) \quad &= \sum_i a_i \sum_j b_j f^{(\beta)}(\mathbf{x}_i + \mathbf{x}_j) = A(B), \end{aligned}$$

where any derivative shift simply moved from the A stencil to the B stencil. \square

As a demonstration consider the composition of the first-order accurate forward-finite difference approximations to the first and second derivatives:

$$(28) \quad f'(x_0) \longrightarrow \frac{f(x_1) - f(x_0)}{h} + \mathcal{O}(h),$$

$$(29) \quad f''(x_0) \longrightarrow \frac{f(x_2) - 2f(x_1) + f(x_0)}{h^2} + \mathcal{O}(h),$$

where the A stencil corresponds to $f'(x_0)$ and the B stencil to $f''(x_0)$. This results in $\mathbf{u} = \{1, 0\}$ and $\mathbf{v} = \{2, 1, 0\}$ as the associated integer vectors with weights $\mathbf{a} = \{1/h, -1/h\}$ and $\mathbf{b} = \{1/h^2, -2/h^2, 1/h^2\}$, respectively. First consider $B(A)$:

$$\begin{aligned} B(A) &= \sum_j \sum_i a_i b_j f(\mathbf{x}_i + \mathbf{x}_j) = \sum_j b_j \left[\frac{1}{h^2} (f(x_{2+j}) - 2f(x_{1+j}) + f(x_{0+j})) \right] \\ &= \frac{1}{h} \left[\frac{1}{h^2} (f(x_3) - 2f(x_2) + f(x_1)) \right] - \frac{1}{h} \left[\frac{1}{h^2} (f(x_2) - 2f(x_1) + f(x_0)) \right] \\ (30) \quad &= \frac{1}{h^3} (-f(x_0) + 3f(x_1) - 3f(x_2) + f(x_3)) \end{aligned}$$

The overall result can then be obtained via the expansions for $f(x_0)$ to $f(x_3)$,

$$\begin{aligned} B(A) &= \frac{1}{h^3} \left[(-\{1, 0, 0, 0, \dots\}, \beta = 0) + 3 \left(\{1, 1, \frac{1}{2}, \frac{1}{6}, \frac{1}{24}, \dots\}, \beta = 0 \right) \right. \\ &\quad \left. - 3 \left(\{1, 2, 2, \frac{4}{3}, \frac{2}{3}, \dots\}, \beta = 0 \right) + \left(\{1, 3, \frac{9}{2}, \frac{9}{2}, \frac{27}{8}, \dots\}, \beta = 0 \right) \right] \\ (31) \quad &= \frac{1}{h^3} \left(\{0, 0, 1, \frac{3}{2}, \dots\}, \beta = 0 \right) = \left(\{1, \frac{3}{2}, \dots\}, \beta = 3 \right), \end{aligned}$$

which corresponds to an $\mathcal{O}(h)$ approximation to $f'''(x_0)$. Derivation of this result using the method shown in (22) can be found in the appendix.

Associativity can be demonstrated in this example via determining the composition $A(B)$:

$$\begin{aligned} A(B) &= \sum_i \sum_j a_i b_j f(\mathbf{x}_i + \mathbf{x}_j) = \sum_i a_i \left[\frac{1}{h} (f(x_{i+1}) - f(x_{i+0})) \right] \\ &= \frac{1}{h^2} \left[\frac{1}{h} (f(x_3) - f(x_2)) \right] - \frac{2}{h^2} \left[\frac{1}{h} (f(x_2) - f(x_1)) \right] + \left[\frac{1}{h} (f(x_1) - f(x_0)) \right] \\ (32) \quad &= \frac{1}{h^3} (-f(x_0) + 3f(x_1) - 3f(x_2) + f(x_3)), \end{aligned}$$

which is the same as (30) and will thus have the approximation and order as (31).

2.2.2. Order of Accuracy. The rate at which the local truncation error, expressed as a function of h , approaches zero as h approaches zero is the *order of accuracy* of the method [13]. In order to show the order of accuracy of the *composed* stencil, we need to introduce the concept of re-targeting. This involves moving a stencil from a target point $\mathbf{y}_0 \neq \mathbf{x}_0$ to the original target point \mathbf{x}_0 . This can be accomplished by taking the Taylor Series of a linear combination, (\mathbf{T}, β) , and accounting for the additional error terms. Recalling that t_α represents the coefficient multiplying the $h^\alpha f^{(\alpha+\beta)}$ term

of the linear combination Taylor Series, the updated series at the original target point \mathbf{x}_0 can be obtained by replacing the original derivatives $f^{(\alpha+\beta)}$ in the sum by their own Taylor Series expanded about the original target point:

$$(33) \quad \sum_{|\alpha| \geq 0} t_\alpha h^\alpha \sum_{|\delta| \geq 0} \frac{(\mathbf{y}_0 - \mathbf{x}_0)^\delta}{\delta!} f^{(\alpha+\beta+\delta)}(\mathbf{x}_0) = \sum_{|\alpha| \geq 0} t_\alpha h^\alpha f^{(\alpha+\beta)}(\mathbf{x}_0) + \sum_{|\alpha| \geq 0} t_\alpha h^\alpha \sum_{|\delta| \geq 1} \frac{(\mathbf{y}_0 - \mathbf{x}_0)^\delta}{\delta!} f^{(\alpha+\beta+\delta)}(\mathbf{x}_0) \longrightarrow (\mathbf{T}, \beta) + (\mathbf{C}_{\mathbf{y}_0 \rightarrow \mathbf{x}_0}, \beta),$$

which demonstrates that re-targeting is simply the addition of the original Taylor series with a correction series given by $(\mathbf{C}_{\mathbf{y}_0 \rightarrow \mathbf{x}_0}, \beta)$. The first non-zero element in $\mathbf{C}_{\mathbf{y}_0 \rightarrow \mathbf{x}_0}$ will be one order higher to the first non-zero element in \mathbf{T} due to $\|(\mathbf{y}_0 - \mathbf{x}_0)^\delta\| \geq h$ when $\delta \geq 1$.

As a demonstration consider re-targeting the one-dimensional, second-order accurate, center-finite-difference stencil of the second derivative at the point $y_0 = x_0 + h$ to the point x_0 . Recall in this case we have $\mathbf{T} = \{1, 0, 1/12, 0, \dots\}$ and $\beta = 2$. Therefore, the correction can be written as

$$(34) \quad \sum_{|\alpha| \geq 0} t_\alpha h^\alpha \sum_{|\delta| \geq 1} \frac{(y_0 - x_0)^\delta}{\delta!} f^{(\alpha+2+\delta)}(x_0) = hf^{(3)}(x_0) + \frac{1}{2}h^2 f^{(4)}(x_0) + \frac{1}{4}h^3 f^{(5)}(x_0) + \dots \longrightarrow (\{0, 1, \frac{1}{2}, \frac{1}{4}, \dots\}, \beta = 2).$$

Following the previous statements, the first non-zero element in the correction is of one order of h higher than the original expansion, which corresponds to the second location in this case.

Adding this to the original series we obtain

$$(35) \quad (\{1, 0, 1/12, 0, \dots\}, \beta = 2) + (\{0, 1, \frac{1}{2}, \frac{1}{4}, \dots\}, \beta = 2) = (\{1, 1, \frac{7}{12}, \frac{1}{4}, \dots\}, \beta = 2),$$

which corresponds to the the second-derivative of $f(x)$ approximated at x_0 but using the stencil centered at $y_0 = x_0 + h$. From this, re-targeting can be thought of approximating a derivative at a point *away* from x_0 and then calculating how well that is an approximation is of the same derivative *at* x_0 .

It is now possible to determine the order of accuracy of stencil composition. Let us take our inner stencil, A , as defined earlier in (19). Using (10), we can write the inner stencil as,

$$(36) \quad \sum_i a_i \left(\sum_{|\alpha| \geq 0} h^\alpha \frac{\mathbf{u}_i^\alpha}{\alpha!} f^{(\alpha+\beta)}(\mathbf{x}_0) \right) = \sum_{|\alpha| \geq 0} t_\alpha h^\alpha f^{(\alpha+\beta)}(\mathbf{x}_0),$$

where t_α denotes the coefficient associated with h^α and takes into account the associated weights a_i .

When applying the outer-stencil, B , the inner stencil is being evaluated away from the target point. Therefore, the inner stencils need to be re-targeted. Using (33), the composition can be written as,

$$(37) \quad B(A) = \sum_j b_j \sum_{|\alpha| \geq 0} t_\alpha h^\alpha f^{(\alpha+\beta)}(\mathbf{x}_j) = \sum_j b_j \sum_{|\alpha| \geq 0} t_\alpha h^\alpha \sum_{|\delta| \geq 0} \frac{(\mathbf{x}_j - \mathbf{x}_0)^\delta}{\delta!} f^{(\alpha+\beta+\delta)}(\mathbf{x}_0)$$

Rearranging the summations on the right hand side we can rewrite the equation above as

$$(38) \quad B(A) = \sum_{|\alpha| \geq 0} t_\alpha h^\alpha \sum_j b_j \sum_{|\delta| \geq 0} \frac{(\mathbf{x}_j - \mathbf{x}_0)^\delta}{\delta!} f^{(\alpha+\beta+\delta)}(\mathbf{x}_0) = \sum_{|\alpha| \geq 0} t_\alpha h^\alpha \sum_{|\delta| \geq 0} t_\delta h^\delta f^{(\alpha+\beta+\delta)}(\mathbf{x}_0),$$

where t_δ denotes the coefficient associated with h^δ and takes into account the associated weights b_j . We will use this result for proving the resulting order of accuracy of a *composed* stencil, demonstrated below.

Lemma 2. *Stencil composition of two stencils A and B with orders of accuracy q_a and q_b , respectively, results in a composed stencil $C = B(A)$ with order of accuracy $q_c = \min(q_a, q_b)$.*

Proof. Let the inner stencil A be an approximation with an order of derivative of p_a and order of accuracy of q_a . Then, we can write A as,

$$(39) \quad \begin{aligned} A &= f^{(p_a)} + \sum_{|\alpha| \geq q_a} t_\alpha h^\alpha f^{(\alpha+p_a)}(\mathbf{x}_0) \longrightarrow (\mathbf{T}_A, \beta = p_a) \\ &\longrightarrow (\{1, 0, \dots, 0, t_{q_a}, \dots\}, \beta = p_a), \end{aligned}$$

where t_{q_a} is the coefficient associated with order of accuracy term h^{q_a} . Similarly, we can write the outer stencil B approximating an order of derivative of p_b and order of accuracy q_b as

$$(40) \quad B \longrightarrow (\mathbf{T}_B, \beta = p_b) \longrightarrow (\{1, 0, \dots, 0, t_{q_b}, \dots\}, \beta = p_b).$$

From (38), we can write the composition $B(A)$ as,

$$B(A) = \sum_{|\alpha| \geq 0} t_\alpha h^\alpha \sum_{|\delta| \geq 0} t_\delta h^\delta f^{(\alpha+\beta+\delta)}(\mathbf{x}_0).$$

Using coefficient vectors \mathbf{T}_A and \mathbf{T}_B the same equation can be written as,

$$(41) \quad B(A) \longrightarrow (\mathbf{T}_A, \beta = p_a) \circ (\mathbf{T}_B, \beta = p_b) \longrightarrow (\mathbf{T}_A \circ \mathbf{T}_B, \beta = p_a + p_b).$$

Recall that \mathbf{T}_A and \mathbf{T}_B are simply short-hand notation for

$$(42) \quad \mathbf{T}_A \longrightarrow \{1 \cdot h^0, 0 \cdot h^1, \dots, 0 \cdot h^{q_a-1}, t_{q_a} h^{q_a}, \dots\},$$

$$(43) \quad \mathbf{T}_B \longrightarrow \{1 \cdot h^0, 0 \cdot h^1, \dots, 0 \cdot h^{q_b-1}, t_{q_b} h^{q_b}, \dots\}.$$

Then the list composition can be written as

$$(44) \quad \begin{aligned} \mathbf{T}_A \circ \mathbf{T}_B &\longrightarrow 1h^0(\{1h^0, 0, \dots, 0, t_{q_b} h^{q_b}, \dots\}) + 0h^1(\{1h^0, 0, \dots, 0, t_{q_b} h^{q_b}, \dots\}) + \dots \\ &+ t_{q_a} h^{q_a}(\{1h^0, 0, \dots, 0, t_{q_b} h^{q_b}, \dots\}) + \dots \end{aligned}$$

If $q_a < q_b$, the first non-unitary element in $B(A)$ would be, $t_{q_a} h^{q_a}$, implying an order of accuracy of q_a . Similarly if $q_b < q_a$, the first non-zero term would be, $t_{q_b} h^{q_b}$, and hence order accuracy being q_b . In the case of $q_a = q_b$, the first non-zero term would be $t_{q_a} h^{q_a} + t_{q_b} h^{q_b}$ and since $q_a = q_b$ this implies the order of accuracy is $q_a = q_b$. This proves that when two stencils with orders of accuracy q_a and q_b respectively are composed, the order of accuracy of the composed stencil is $\min(q_a, q_b)$. \square

Another observation can be made here regarding the coefficient of the leading order error term in the composed stencil, written as a Proposition below.

Proposition 1. *Stencil composition of two stencils A and B with orders of accuracy q_a and q_b , respectively, with coefficients of the leading order error terms being t_{q_a} and t_{q_b} , respectively, leads to a composed stencil $C = B(A)$ with order of accuracy $q_c = \min(q_a, q_b)$ and a leading-order error coefficient t_{q_c} equal to,*

$$t_{q_c} = \begin{cases} t_{q_a} & \text{if } q_c = q_a, \\ t_{q_b} & \text{if } q_c = q_b, \\ t_{q_a} + t_{q_b}, & \text{if } q_c = q_a = q_b. \end{cases}$$

As an example, we compose a second-order accurate first derivative stencil with a fourth-order accurate first derivative stencil to obtain a second-derivative stencil. As a reminder, the second-order accurate first derivative stencil (17) is

$$f'(x_0) \longrightarrow \frac{f(x_1) - f(x_{-1})}{2h} + \mathcal{O}(h^2) \longrightarrow (\{1, 0, \frac{1}{6}, 0, \dots\}, \beta = 1),$$

and the fourth-order accurate first derivative stencil can be written as

$$(45) \quad \begin{aligned} f'(x_0) &\longrightarrow \frac{8f(x_1) - f(x_2) + f(x_{-2}) - 8f(x_{-1})}{12h} + \mathcal{O}(h^4) \\ &\longrightarrow \left(\{1, 0, 0, 0, \frac{-1}{30}, \dots\}, \beta = 1 \right). \end{aligned}$$

Let the outer-stencil correspond to second-order accurate approximation to $f'(x_0)$ while the inner-stencil is the fourth-order accurate approximation to $f'(x_0)$. This results in $\mathbf{u} = \{1, 2, -2, -1\}$ and $\mathbf{v} = \{1, -1\}$ as the associated

integer vectors with weights $\mathbf{a} = \{8/12h, -1/12h, 1/12h, -8/12h\}$ and $\mathbf{b} = \{1/h, -1/h\}$, respectively. Performing the composition we get

$$\begin{aligned}
 B(A) &= \sum_j^2 \sum_i^4 a_i b_j f(\mathbf{x}_i + \mathbf{x}_j) \\
 &= \sum_j^2 b_j \left[\frac{1}{12h} (8f(x_{1+j}) - f(x_{2+j}) + f(x_{-2+j}) - 8f(x_{-1+j})) \right] \\
 &= \frac{1}{h} \left[\frac{1}{12h} (8f(x_2) - f(x_3) + f(x_{-1}) - 8f(x_0)) \right] \\
 &\quad - \frac{1}{h} \left[\frac{1}{12h} (8f(x_0) - f(x_1) + f(x_{-3}) - 8f(x_{-2})) \right] \\
 (46) \quad &= \frac{1}{12h^2} (-f(x_{-3}) + 8f(x_{-2}) + f(x_{-1}) - 16f(x_0) + f(x_1) + 8f(x_2) - f(x_3))
 \end{aligned}$$

The overall result can then be obtained via the expansions for $f(x_{-3})$ to $f(x_3)$,

$$\begin{aligned}
 B(A) &= \frac{1}{12h^2} \left[- \left(\{1, 3, \frac{9}{2}, \frac{9}{2}, \frac{27}{8}, \dots\}, \beta = 0 \right) + 8 \left(\{1, -2, 2, \frac{-4}{3}, \frac{2}{3}, \dots\}, \beta = 0 \right) \right. \\
 &\quad + \left(\{1, -1, \frac{1}{2}, \frac{-1}{6}, \frac{1}{24}, \dots\}, \beta = 0 \right) - 16 \left(\{1, 0, 0, 0, 0, \dots\}, \beta = 0 \right) \\
 &\quad + \left(\{1, 1, \frac{1}{2}, \frac{1}{6}, \frac{1}{24}, \dots\}, \beta = 0 \right) + 8 \left(\{1, 2, 2, \frac{4}{3}, \frac{2}{3}, \dots\}, \beta = 0 \right) \\
 &\quad \left. - \left(\{1, -3, \frac{9}{2}, \frac{-9}{2}, \frac{27}{8}, \dots\}, \beta = 0 \right) \right] \\
 (47) \quad &= \frac{1}{12h^2} (\{0, 0, 12, 0, 2, \dots\}, \beta = 0) = \left(\{1, 0, \frac{1}{6}, \dots\}, \beta = 2 \right),
 \end{aligned}$$

Upon composing a fourth-order accurate stencil with a second order accurate stencil the leading order error term is in the location corresponding to h^2 and thus the composition order of accuracy is $\min(2, 4)$, demonstrating Lemma 2. This also demonstrates Proposition 1, as the coefficient of error term in the composed stencil is $\frac{1}{6}$ which matches the coefficient of the error term in second-order accurate stencil in (17).

2.3. Higher-dimensional Stencil Composition. Another benefit of using stencil composition to obtain higher order derivatives is its possibility of extension to higher dimensions. By performing stencil composition in two or three dimensions one can easily obtain higher-order mixed derivatives. When two stencils in different dimensions are composed the resulting stencil is simply the outer product of the two stencils, demonstrated using two-dimensional examples below.

If we have two stencils \mathbf{T}_{X_i} and \mathbf{T}_{Y_j} in the x and y directions, respectively, approximating derivative of orders p_x and p_y , such that

$$(48) \quad f^{(p_x)}(\mathbf{x}_i) \longrightarrow (\mathbf{T}_{X_i}, \beta_x = p_x) \text{ and } f^{(p_y)}(\mathbf{y}_j) \longrightarrow (\mathbf{T}_{Y_j}, \beta_y = p_y),$$

then the composition of the two stencils yields a mixed derivative equal to the outer product of the two stencils,

$$(49) \quad f^{(p_x, p_y)}(\mathbf{x}_i, \mathbf{y}_j) \longrightarrow (\mathbf{T}_{X_i} \otimes \mathbf{T}_{Y_j}, \beta_x = p_x, \beta_y = p_y)$$

As an example, let us compose first derivative stencils in the x and y direction to obtain the mixed derivative $f^{(1,1)}(x, y)$. Let $\mathbf{x}_0 = (x_0, y_0)$ be the target point. We can write the stencils of second-order accurate first derivative stencils in each direction thusly,

$$(50) \quad f'(x_0) \longrightarrow (\{1, 0, \frac{1}{6}, 0, \dots\}, \beta_x = 1),$$

$$(51) \quad f'(y_0) \longrightarrow (\{1, 0, \frac{1}{6}, 0, \dots\}, \beta_y = 1).$$

Taking the outer product we obtain

$$(52) \quad (\{1, 0, \frac{1}{6}, 0, \dots\} \otimes \{1, 0, \frac{1}{6}, 0, \dots\}, \beta_x = 1, \beta_y = 1) = \left(\begin{bmatrix} 1 & 0 & \frac{1}{6} & 0 & \dots \\ 0 & 0 & 0 & 0 & \dots \\ \frac{1}{6} & 0 & \frac{1}{36} & 0 & \dots \\ 0 & 0 & 0 & 0 & \dots \\ \vdots & \vdots & \vdots & \vdots & \ddots \end{bmatrix}, \beta_x = 1, \beta_y = 1 \right),$$

which can be written in the expanded form as the following,

$$(53) \quad f^{(1,1)}(\mathbf{x}_i, \mathbf{y}_j) \longrightarrow f^{(1,1)}(x_0, y_0) + \frac{1}{6}h_x^2 \cdot f^{(3,1)}(x_0, y_0) + \frac{1}{6}h_y^2 \cdot f^{(1,3)}(x_0, y_0) + \frac{1}{36}h_x^2 h_y^2 \cdot f^{(3,3)}(x_0, y_0) + \dots,$$

where h_x and h_y are the spacing in the lattice in x and y directions respectively. For simplicity, assume that $h_x = h_y = h$. We can then rewrite the equation above as following,

$$(54) \quad f^{(1,1)}(\mathbf{x}_i, \mathbf{y}_j) \longrightarrow f^{(1,1)}(a, b) + \frac{1}{6}h^2 \cdot f^{(3,1)}(a, b) + \frac{1}{6}h^2 \cdot f^{(1,3)}(a, b) + \frac{1}{36}h^4 \cdot f^{(3,3)}(a, b) + \dots$$

Note that the error term is proportional to $\mathcal{O}(h^2)$, therefore the composed stencil is also second-order accurate.

Lets us now compose two stencils of different order of accuracies in two dimensions. For instance, composition of a fourth-order accurate stencil in the x -direction and second-order accurate stencil in the y -direction,

$$(55) \quad f'(a) \longrightarrow (\{1, 0, 0, 0, \frac{-1}{30}, 0, \dots\}, \beta_x = 1),$$

$$(56) \quad f'(b) \longrightarrow (\{1, 0, \frac{1}{6}, 0, \frac{1}{120}, \dots\}, \beta_y = 1),$$

will give us the following,

$$(57) \quad f^{(1,1)}(a, b) \longrightarrow \left(\begin{bmatrix} 1 & 0 & \frac{1}{6} & 0 & \frac{1}{120} & \dots \\ 0 & 0 & 0 & 0 & 0 & \dots \\ 0 & 0 & 0 & 0 & 0 & \dots \\ 0 & 0 & 0 & 0 & 0 & \dots \\ \frac{-1}{30} & 0 & \frac{-1}{180} & 0 & \frac{-1}{3600} & \dots \\ \vdots & \vdots & \vdots & \vdots & \vdots & \ddots \end{bmatrix}, \beta_x = 1, \beta_y = 1 \right).$$

In this case the highest order error term would be $\frac{1}{6}h^2 \cdot f^{(1,3)} \in \mathcal{O}(h^2)$, demonstrating that the composed stencil is second-order accurate. Both of the examples illustrate that Lemma 2 still holds true for higher dimensional composition.

3. NUMERICAL EXAMPLES

In this section the convergence of one- and two-dimensional examples, in addition to the bi-harmonic equation is presented. In addition to verification of the expected order-of-accuracy, we will also determine the coefficient associated with error. All MATLAB code for the examples is available in the supplementary materials.

3.1. One-dimensional Example. Begin by considering the one-dimensional function $f(x) = \sin(x) \cos(x)$. We will approximate the third-derivative of this function, $f^{(3)}(x) = 4\sin^2(x) - 4\cos^2(x)$, via the composition of second-order accurate first-derivative and second-derivative stencils given by $\mathbf{u} = \{1, -1\}$ and $\mathbf{v} = \{1, 0, -1\}$ with weights of $\mathbf{a} = \{1/h, -1/h\}$ and $\mathbf{b} = \{1/h^2, -2/h^2, 1/h^2\}$, respectively. This results in a series for the first-derivative of

$$(58) \quad f'(x) \longrightarrow (\{1, 0, \frac{1}{6}, 0, \frac{1}{120}, \dots\}, \beta = 1)$$

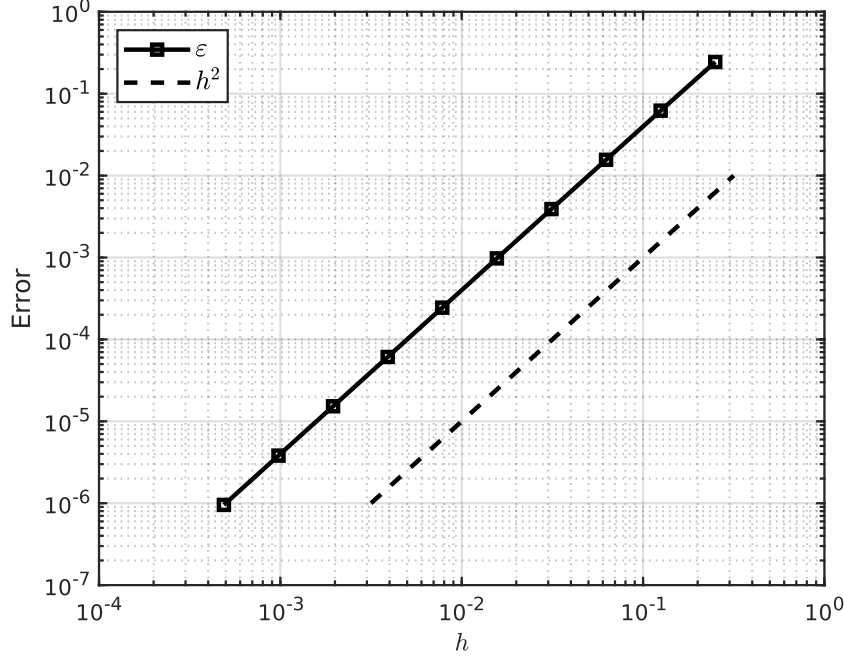


FIGURE 1. The error evaluated at $x = \pi$ between the third-derivative of $f(x) = \sin(x)\cos(x)$ and a finite-difference stencil obtained via composition of second-order accurate approximations to the first- and second-derivatives.

while the second-derivative series is

$$(59) \quad f''(x) \longrightarrow (\{1, 0, \frac{1}{12}, 0, \frac{1}{360}, \dots\}, \beta = 2).$$

We expect that the composition will result in an $\mathcal{O}(h^2)$ -accurate stencil with a leading-order error coefficient of $1/6 + 1/12 = 1/4$, or in other words we expect that the error will scale as $\frac{1}{4}h^2$, which can be verified from the Taylor-Series of the composition:

$$(60) \quad f^{(3)}(x) \longrightarrow (\{1, 0, \frac{1}{4}, 0, \frac{1}{40}, \dots\}, \beta = 3).$$

The error evaluated at $x = \pi$ as a function of grid-spacing h is shown in Fig. 1. As expected, the rate-of-convergence equals that of the prediction. To verify the coefficient associated with this convergence we fit a line in log-log space:

$$(61) \quad \log \varepsilon = p \log h + \log C,$$

where ε is the error, p is the calculated order of convergence and C is the leading-order coefficient. Fitting the data results in $p = 1.9976 \approx 2$, which matches the expected order of convergence and $C \approx 3.9432$. From the Taylor-Series of the approximation, (60), the coefficient of the error should equal $\frac{1}{4}f^{(5)}(\pi) = 4$, which is very close to the calculated value.

3.2. Two-dimensional Example. Let us now consider a two-dimensional function, $f(x, y) = \sin(x)\cos(y) + \cos(x)\sin(y)$ where we are interested approximating $f^{4,3}(x)$ with fourth-order accuracy. As before we will verify the order of accuracy and the associated coefficient. To build the overall stencil we will be using multiple compositions. First, a centered, fourth-order accurate discretization of the second-derivative is composed with itself to obtain a fourth-order accurate representation of the fourth-derivative:

$$(62) \quad f^{(4)}(\mathbf{x}) \longrightarrow (\{1, 0, 0, 0, -\frac{1}{45}, 0, -\frac{1}{504}, \dots\}, \beta = 4).$$

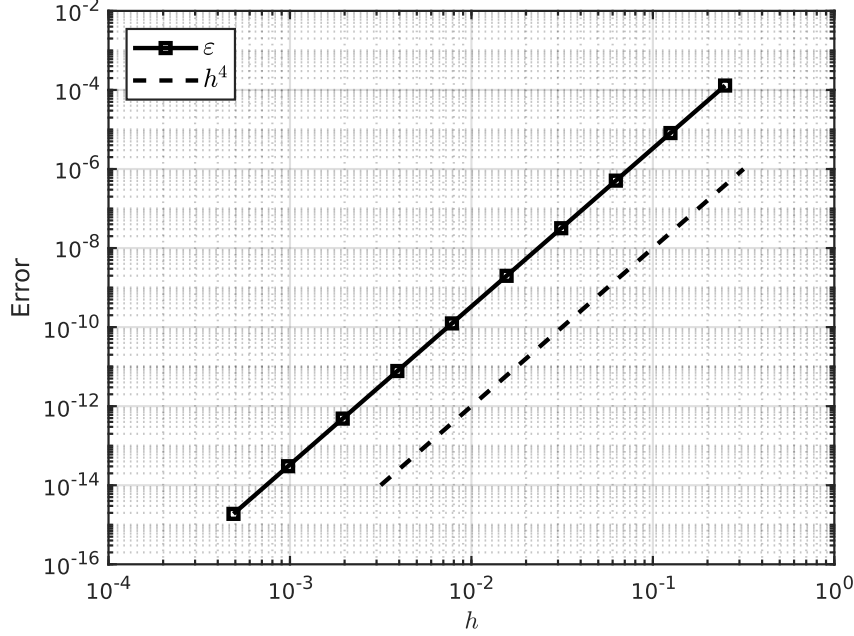


FIGURE 2. The error of approximating $f^{(4,3)}(x,y)$, where $f(x,y) = \sin(x)\cos(y) + \cos(x)\sin(y)$, obtained by composing two fourth-order accurate second derivative stencils in x and fourth-order accurate first and second derivative stencils in y , evaluated at $(x,y) = (2\pi, \pi/3)$. The dashed lines indicates a fourth-order accurate solution.

Second, a centered fourth-order accurate discretization of the first-derivative is composed with the fourth-order accurate second derivative approximation:

$$(63) \quad f^{(3)}(\mathbf{x}) \longrightarrow (\{1, 0, 0, 0, -\frac{2}{45}, 0, -\frac{5}{1008}, \dots\}, \beta = 3).$$

Composing the fourth-derivative in the x -direction with the third-derivative in the y -direction results in

$$(64) \quad f^{(4,3)}(\mathbf{x}) \longrightarrow \left(\begin{bmatrix} 1 & 0 & 0 & 0 & -\frac{2}{45} & \dots \\ 0 & 0 & 0 & 0 & 0 & \dots \\ 0 & 0 & 0 & 0 & 0 & \dots \\ 0 & 0 & 0 & 0 & 0 & \dots \\ -\frac{1}{45} & 0 & 0 & 0 & \frac{2}{2025} & \dots \\ \vdots & \vdots & \vdots & \vdots & \vdots & \ddots \end{bmatrix}, \beta_x = 4, \beta_y = 3 \right),$$

which corresponds to $f^{4,3}(\mathbf{x}) + h^4 \left(-\frac{1}{45}f^{(8,3)}(\mathbf{x}) - \frac{2}{45}f^{(4,7)}(\mathbf{x}) \right) + \dots$.

The error between the exact solution, $f^{(4,3)}(x,y) = \sin(x)\sin(y) - \cos(x)\cos(y)$, and the approximation computed via the composed finite-difference stencil at location $\mathbf{x} = (2\pi, \pi/3)$ is shown in Fig. 2. Following (61) the calculated convergence rate is 3.9997 while $C = 3.324 \times 10^{-2}$, close to the expected value of $-\left(f^{(8,3)}(\mathbf{x}) + 2f^{(4,7)}(\mathbf{x})\right)/45 = 1/30$.

3.3. Biharmonic Equation. Finally, consider the solution of a linear system arising from the discretization of a high-order differential equation. Specifically, we consider solutions of the biharmonic equation, which is a fourth-order linear partial differential equation with applications in various areas of mechanics, including the theory of elasticity and flow of viscous fluids [17]. In two-dimensions, the biharmonic of a function $f(x,y)$ can be written as

$$(65) \quad \Delta(\Delta f) = \frac{\partial^4 f}{\partial x^4} + 2\frac{\partial^4 f}{\partial x^2 \partial y^2} + \frac{\partial^4 f}{\partial y^4} = g(x,y),$$

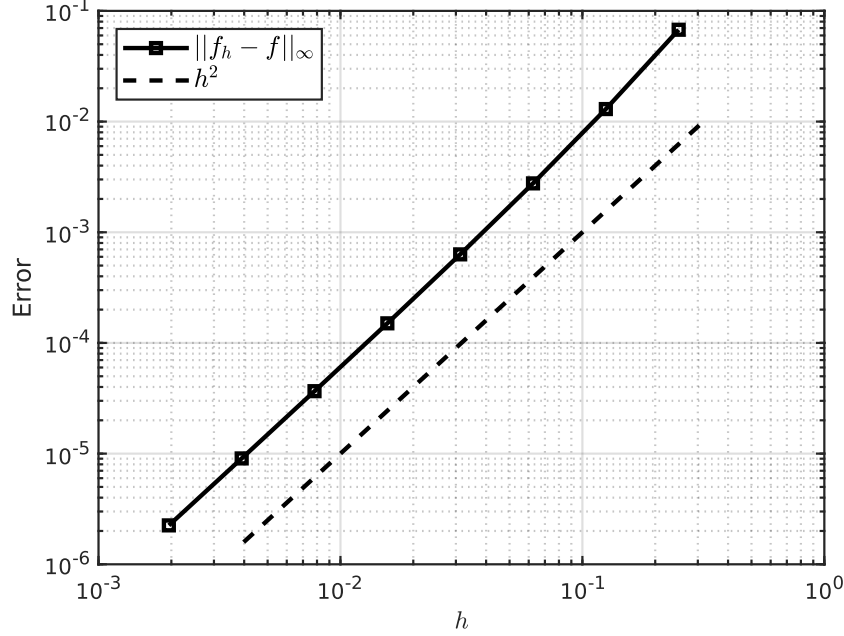


FIGURE 3. Convergence test of biharmonic boundary value problem. Show is the l_∞ -norm of the error in the domain versus grid spacing h for $\Delta(\Delta f) = 4\pi^4 \sin(\pi x) \sin(\pi y)$ obtained by composition of second-order accurate stencils evaluated on a unit square domain $\{0 \leq x \leq 1, 0 \leq y \leq 1\}$ with appropriate boundary conditions. The dashed line indicates slope for a second-order accurate solution, matching the expected result.

with appropriate boundary conditions on a bounded domain [9] and where $g(x, y)$ is the problem-specific forcing function.

For our numerical experiment we consider a simply supported rectangular plate with sides of unit length $\{0 \leq x \leq 1, 0 \leq y \leq 1\}$ and a given solution of $f(x, y) = \sin(\pi x) \sin(\pi y)$. This results in boundary conditions of [2]

$$(66a) \quad f = 0, \frac{\partial^2 f}{\partial x^2} = 0 \quad \text{for } x = 0 \text{ and } x = 1, \text{ and}$$

$$(66b) \quad f = 0, \frac{\partial^2 f}{\partial y^2} = 0 \quad \text{for } y = 0 \text{ and } y = 1$$

and a forcing function of

$$(67) \quad g(x, y) = 4\pi^4 \sin(\pi x) \sin(\pi y).$$

There are two ways we can make use of composition to obtain the stencil for the biharmonic equation. In the first method we can use composition to discretize the middle equation of (65). While this is straight-forward to accomplish, it requires that the spatial dimension of the underlying grid be taken into account as there will be additional terms in the z -direction if this is a three-dimensional problem instead of a two-dimensional one. An alternative is to create a single Laplacian stencil and compose this stencil with itself, *i.e.* using stencil composition to compute the left-hand side equation of (65) directly. From an implementation point-of-view this second approach is much more attractive as any dimension-dependence will already be taken into account when forming the Laplacian stencil. Additionally, as both methods will result in the same stencil, so the second approach is the one used here.

The error results in the l_∞ -norm for the given problem are shown in Fig. 3 where the discretization of the Laplacian was achieved using second-order accurate stencils. Based on this, we expect that the discretization of the biharmonic equation will maintain this second-order accuracy, which is verified by calculating the rate-of-convergence of the test.

4. DISCUSSION AND CONCLUSION

In this work we make use of composition to form finite difference stencils which can then be used to numerically evaluate derivatives and solve partial differential equations. In stencil composition, two stencils with arbitrary derivative-orders are composed to obtain a stencil with a derivative-order equal to the sum of each individual stencil approximation. We represent stencils for various orders of derivative as stencil vectors, with the elements being the coefficients of the truncation error terms, allowing for the determination of the leading-order error term of the composed stencil. We show that stencil composition is associative and prove that the order-of-accuracy of the composed stencil will never fall below the lowest-order accuracy of the stencils being composed. Numerical examples, both in one- and two-dimensions, verify our findings regarding order of accuracy via convergence tests. A PDE application is also shown, wherein a boundary value problem involving the biharmonic equation is discretized using the composition of two Laplacian stencils, and the convergence rate is verified.

There are several aspects of the work that must also be discussed. First, this method will *not* result in the most compact stencil except in cases where composition is used to obtain derivatives in higher-dimensions. If not careful this may result in a decoupling of solutions in adjacent nodes, similar to the checkerboard effect in collocated Navier-Stokes methods [18, 6].

Second, the work here only holds if the inner stencils for a composition do not vary from location-to-location in the outer stencil. For example, consider composing two finite difference stencils of the second-derivative in a domain. At the boundary it may be tempting to mix one-sided stencils with center-stencils. This is not advised, as the composition is no longer between a single inner and single outer function, but different functions, which creates unpredictable results. As a demonstration consider the composition of first-derivative approximations to obtain a second-derivative stencil. Let the outer stencil be given by $\mathbf{u} = \{1, -1\}$ with weights $\mathbf{a} = \{1/(2h), -1/(2h)\}$. At location x_1 the standard stencil is used: $\mathbf{v}_1 = \mathbf{u}$ and $\mathbf{b}_1 = \mathbf{a}$. At location x_{-1} a forward-approximation is used: $\mathbf{v}_{-1} = \{1, 0, -1\}$ and $\mathbf{b}_{-1} = \{-1/(2h), 2/h, -3/(2h)\}$. Composition using these results in a series of $(\{-1/2, 0, -1/24, \dots\}, \beta = 2)$, which is clearly not an approximation to the second-derivative. Other combinations may result in the negative of the expected result, zero, or something else completely. Note that it is perfectly acceptable to mix approximations at different target locations. For example, at a domain boundary we can use all one-sided approximations for the inner stencil and center-approximations at the interior.

With these caveats in mind, our results demonstrate that it is possible to construct complex differential stencils with guaranteed accuracy via the composition of lower-derivative approximations. This is the first step towards facilitating the formation of large-scale linear systems of arbitrary partial differential equations in a systematic and automatic manner. Future work will include the implementation of these concepts into numerical tools for the wider community, and an investigation of the composition between interpolation and differentiation operations, similar to those in the Closest Point Method.

REFERENCES

- [1] Daniel Appelö and N Anders Petersson. “A stable finite difference method for the elastic wave equation on complex geometries with free surfaces”. In: *Communications in Computational Physics* 5.1 (2009), pp. 84–107.
- [2] M Arad, A Yakhot, and G Ben-Dor. “A highly accurate numerical solution of a biharmonic equation”. In: *Numerical Methods for Partial Differential Equations: An International Journal* 13.4 (1997), pp. 375–391.
- [3] Erik Burman and Peter Hansbo. “Fictitious domain finite element methods using cut elements: II. A stabilized Nitsche method”. In: *Applied Numerical Mathematics* 62.4 (2012), pp. 328–341.
- [4] Yujia Chen and Colin B. Macdonald. “The Closest Point Method and multigrid solvers for elliptic equations on surfaces”. In: *SIAM J. Sci. Comput.* 37.1 (2015).
- [5] Ismet Demirdžić and Samir Muzaferija. “Finite volume method for stress analysis in complex domains”. In: *International journal for numerical methods in engineering* 37.21 (1994), pp. 3751–3766.
- [6] Filippo Maria Denaro. “A 3D second-order accurate projection-based Finite Volume code on non-staggered, non-uniform structured grids with continuity preserving properties: Application to buoyancy-driven flows”. In: *International Journal for Numerical Methods in Fluids* 52 (Oct. 2006), pp. 393–432. DOI: 10.1002/fld.1185.
- [7] Kenneth Duru and Kristoffer Virta. “Stable and high order accurate difference methods for the elastic wave equation in discontinuous media”. In: *Journal of Computational Physics* 279 (2014), pp. 37–62.
- [8] Charles Elliott. “An Eulerian level set method for partial differential equations on evolving surfaces”. In: *Comput. Vis. Sci.* 13 (2008), pp. 17–22.

- [9] William Ford. *Numerical linear algebra with applications: Using MATLAB*. Academic Press, 2014.
- [10] Jingfeng Gong et al. “An unstructured finite-volume method for transient heat conduction analysis of multi-layer functionally graded materials with mixed grids”. In: *Numerical Heat Transfer, Part B: Fundamentals* 63.3 (2013), pp. 222–247.
- [11] Anita Hansbo and Peter Hansbo. “An unfitted finite element method, based on Nitsche’s method, for elliptic interface problems”. In: *Computer methods in applied mechanics and engineering* 191.47-48 (2002), pp. 5537–5552.
- [12] Peter Hansbo, Mats G Larson, and Sara Zahedi. “A cut finite element method for a Stokes interface problem”. In: *Applied Numerical Mathematics* 85 (2014), pp. 90–114.
- [13] Colin B. Macdonald. “The closest point method for time-dependent processes on surfaces”. PhD thesis. Dept. of Mathematics: Simon Fraser University, 2008.
- [14] Colin B. Macdonald and Steven J. Ruuth. “Level set equations on surfaces via the Closest Point Method”. In: *J. Sci. Comput.* 35.2–3 (2008), pp. 219–240.
- [15] Colin B. Macdonald and Steven J. Ruuth. “The Implicit Closest Point Method for the Numerical Solution of Partial Differential Equations on Surfaces”. In: *SIAM J. Sci. Comput.* 31.6 (2009), pp. 4330–4350.
- [16] Luke Olsen, Philip K Maini, and Jonathan A Sherratt. “Spatially varying equilibria of mechanical models: Application to dermal wound contraction”. In: *Mathematical biosciences* 147.1 (1998), pp. 113–129.
- [17] A. P. S. Selvadurai. *Partial Differential Equations in Mechanics 2: The Biharmonic Equation, Poisson’s Equation*. Berlin: Springer, 2000.
- [18] Tony W. H. Sheu and R. K. Lin. “AN INCOMPRESSIBLE NAVIER-STOKES MODEL IMPLEMENTED ON NONSTAGGERED GRIDS”. In: *Numerical Heat Transfer, Part B: Fundamentals* 44.3 (2003), pp. 277–394. DOI: 10.1080/713836379. eprint: <https://doi.org/10.1080/713836379>. URL: <https://doi.org/10.1080/713836379>.
- [19] HA Stone. “A simple derivation of the time-dependent convective-diffusion equation for surfactant transport along a deforming interface”. In: *Physics of Fluids A: Fluid Dynamics* 2.1 (1990), pp. 111–112.
- [20] Ping Tang et al. “Phase separation patterns for diblock copolymers on spherical surfaces: A finite volume method”. In: *Physical Review E* 72.1 (2005), p. 016710.
- [21] Li Tian, Colin B Macdonald, and Steven J Ruuth. “Segmentation on surfaces with the closest point method”. In: *2009 16th IEEE International Conference on Image Processing (ICIP)*. IEEE. 2009, pp. 3009–3012.
- [22] Siyang Wang, Kristoffer Virta, and Gunilla Kreiss. “High order finite difference methods for the wave equation with non-conforming grid interfaces”. In: *Journal of Scientific Computing* 68.3 (2016), pp. 1002–1028.

APPENDIX A. DERIVATION OF FIRST-ORDER ACCURATE THIRD DERIVATIVE STENCIL USING STENCIL COMPOSITION

If stencil A corresponds to $f'(x_0)$,

$$f'(x_0) \longrightarrow \frac{f(x_1) - f(x_0)}{h} + \mathcal{O}(h),$$

and, stencil B corresponds to $f''(x_0)$,

$$f''(x_0) \longrightarrow \frac{f(x_2) - 2f(x_1) + f(x_0)}{h^2} + \mathcal{O}(h).$$

This results in $\mathbf{u} = \{1, 0\}$ and $\mathbf{v} = \{2, 1, 0\}$ as the associated integer vectors with weights $\mathbf{a} = \{1/h, -1/h\}$ and $\mathbf{b} = \{1/h^2, -2/h^2, 1/h^2\}$, respectively.

The composition $B(A)$ can thus be derived in the following way,

$$\begin{aligned}
B(A) &= \sum_j \sum_i a_i b_j \left(\sum_{|\alpha| \geq 0} h^\alpha \frac{(\mathbf{u}_i + \mathbf{v}_j)^\alpha}{\alpha!} f^{(\alpha)}(\mathbf{x}_0) \right) \\
&= \sum_j b_j \left[\frac{1}{h} \left(\sum_{|\alpha| \geq 0} h^\alpha \frac{(1 + \mathbf{v}_j)^\alpha}{\alpha!} f^{(\alpha)}(\mathbf{x}_0) \right) - \frac{1}{h} \left(\sum_{|\alpha| \geq 0} h^\alpha \frac{\mathbf{v}_j^\alpha}{\alpha!} f^{(\alpha)}(\mathbf{x}_0) \right) \right] \\
&= \frac{1}{h} \left[\frac{1}{h^2} \left(\sum_{|\alpha| \geq 0} h^\alpha \frac{3^\alpha}{\alpha!} f^{(\alpha)}(\mathbf{x}_0) \right) - \frac{2}{h^2} \left(\sum_{|\alpha| \geq 0} h^\alpha \frac{2^\alpha}{\alpha!} f^{(\alpha)}(\mathbf{x}_0) \right) + \frac{1}{h^2} \left(\sum_{|\alpha| \geq 0} h^\alpha \frac{1^\alpha}{\alpha!} f^{(\alpha)}(\mathbf{x}_0) \right) \right] \\
&\quad - \frac{1}{h} \left[\frac{1}{h^2} \left(\sum_{|\alpha| \geq 0} h^\alpha \frac{2^\alpha}{\alpha!} f^{(\alpha)}(\mathbf{x}_0) \right) - \frac{2}{h^2} \left(\sum_{|\alpha| \geq 0} h^\alpha \frac{1^\alpha}{\alpha!} f^{(\alpha)}(\mathbf{x}_0) \right) + \frac{1}{h^2} \left(\sum_{|\alpha| \geq 0} h^\alpha \frac{0^\alpha}{\alpha!} f^{(\alpha)}(\mathbf{x}_0) \right) \right] \\
&= \frac{1}{h^3} \sum_{|\alpha| \geq 0} h^\alpha \frac{3^\alpha - 3(2)^\alpha + 3}{\alpha!} f^{(\alpha)}(\mathbf{x}_0) - \frac{1}{h^3} f(\mathbf{x}_0) \\
&\longrightarrow \frac{1}{h^3} (\{0, 0, 0, 1, \frac{3}{2}, \frac{5}{4}, \dots\}, \beta = 0) = (\{1, \frac{3}{2}, \frac{5}{4}, \dots\}, \beta = 3).
\end{aligned}$$